Nutrient Sensing Using Chip Scale Electrophoresis and *In Situ* Soil Solution Extraction

Zhen Xu, Xinran Wang, Robert J. Weber, *Fellow, IEEE*, Ratnesh Kumar, *Fellow, IEEE*, and Liang Dong

***Abstract*— This paper reports an electrophoresis-based microfluidic ion nutrient sensor for the detection of anions in soil solution samples. The sensor is able to analyze the concentration of various anions in extracted soil solutions with high sensitivity as well as high specificity, while it is an approach requiring no labels. The electrophoretic microchip integrates a pair of in-plane conductivity detection microelectrodes. A programmable high voltage power supply unit was designed to achieve precise control over voltage potentials needed for sample and buffer injection and ion separation. An electrical conductivity detector was designed to extract and process the changes in conductivity due to the arrivals of separated anions at the electrodes at various times. An arrival time serves to identify an anionic species, while the peak height indicates the concentration. A soil water extraction device was also designed to extract the soil solution analyte from the bulk soil, by applying vacuum suction. Only a minute amount of solution (on the order of μL) is needed for the electrophoretic measurement. Extracted soil solutions were analyzed for ionic concentrations to demonstrate the feasibility of using this microfluidic sensor, showing a limit of detection of about 7.25 μM.**

***Index Terms*— Microfluidics, MEMS, electrophoresis, soil sensor, nitrate detection.**

I. Introduction

SENSORS-ENABLED nutrient management for sustainable agriculture is of great societal interest [1]–[4]. In fact, "managing the nitrogen-cycle" is one of the 14 grand challenges put forth by the U.S. National Academy of Engineering. By measuring the available plant nutrients in soil, a more precise nutrient application can be achieved in farming [5], [6]. Sensing the changes in the nutrient ion concentrations is vital for providing the nutrient-sufficient conditions for a maximal plant growth and yield [7]. Therefore, a soil nutrient sensor is important for optimizing nutrient management.

Over the past two decades, many types of soil sensors have been developed to monitor soil properties, including soil moisture [8], [9], pH [10], temperature [11], heavy metal [12], and nutrients [14]. These span various measurement techniques include electrical [8], [14], electromagnetic [15], optical [16], radiometric [17], mechanical [18], acoustic [19], or electrochemical [20]. For the detection of nutrient ions in the soil, common measurement practices include the use of ion chromatography [21], spectrophotometry [22], ion-selective electrodes (ISEs), and electrochemical sensors [23]. Among these, chromatography and spectrophotometry are limited to laboratory settings, while the goal here is design of affordable sensors for site-specific and real-time measurements. ISE-based sensors are field deployable and can convert the activity of a specific ion in a solution into an electrical signal [24]. They, however, rely on specific ion-selective membranes that may degrade over time or may not even be available for certain ions (e.g., for phosphorous ions PO_4^{3-}). Enzymatic electrochemical sensors, using an ion-specific enzyme for molecular recognition, have also been developed to realize detection of a specific ion [25]. Similar to ISEs, this type of sensors are affected by their life time and the availability of the ion-specific enzymes.

To address the issues of sensor life and stability, limited by the recognition agent employed, here we present a label-free design based on the electrophoretic separation of ions and electrical measurements of the conductivity at the end of the electrophoretic channel. There exist other prior applications of electrophoretic separation based sensing. For example, capillary electrophoresis has been used for DNA separation [26], monitoring chemical reactions [27], biomolecules analysis [28], and clinical diagnostics [29]. These applications rely on the fact that bio-particles exhibit different mobility characteristics under an electric potential [30]. The commercial electrophoresis instruments with classic capillaries are often equipped with optical absorption or fluorescence detectors [31]–[34] and allow for a single-molecule level sensitivity, but are bulky and not meant for field applications [35]. Keeping miniaturization and portability in mind, microfluidic devices for chemical analysis and biological assays have recently received considerable attention [36]. In particular, microchip-scale electrophoresis for separation and detection has been studied for many applications and is considerably compact [37]–[40]. In contrast to the commercial electrophoresis instruments, the microchip-based electrophoresis devices integrate simple and effective electrical detection methods [41]. This allows downscaling the detector size without scarifying sensitivity. While many microfluidic electrophoretic devices have been reported as cited above, the application to soil nutrient detection remains limited.

This paper reports a microfluidic electrophoretic nutrient sensor system capable of separating and quantifying inorganic anions in minute (micro-liter) amounts of soil solution samples. A vacuum suction-based soil solution extraction unit

Manuscript received April 6, 2017; accepted May 8, 2017. Date of publication May 16, 2017; date of current version June 23, 2017. This work was supported in part by the U.S. National Science Foundation under Grant CCF-1331390 and Grant IIP-1602089 and in part by the Regents Innovation Fund at the Iowa State University. The associate editor coordinating the review of this paper and approving it for publication was Prof. Sang-Seok Lee. *(Corresponding author: Liang Dong.)*

The authors are with the Department of Electrical and Computer Engineering, Iowa State University, Ames, IA 50011 USA (e-mail: ldong@iastate.edu).

Digital Object Identifier 10.1109/JSEN.2017.2704918

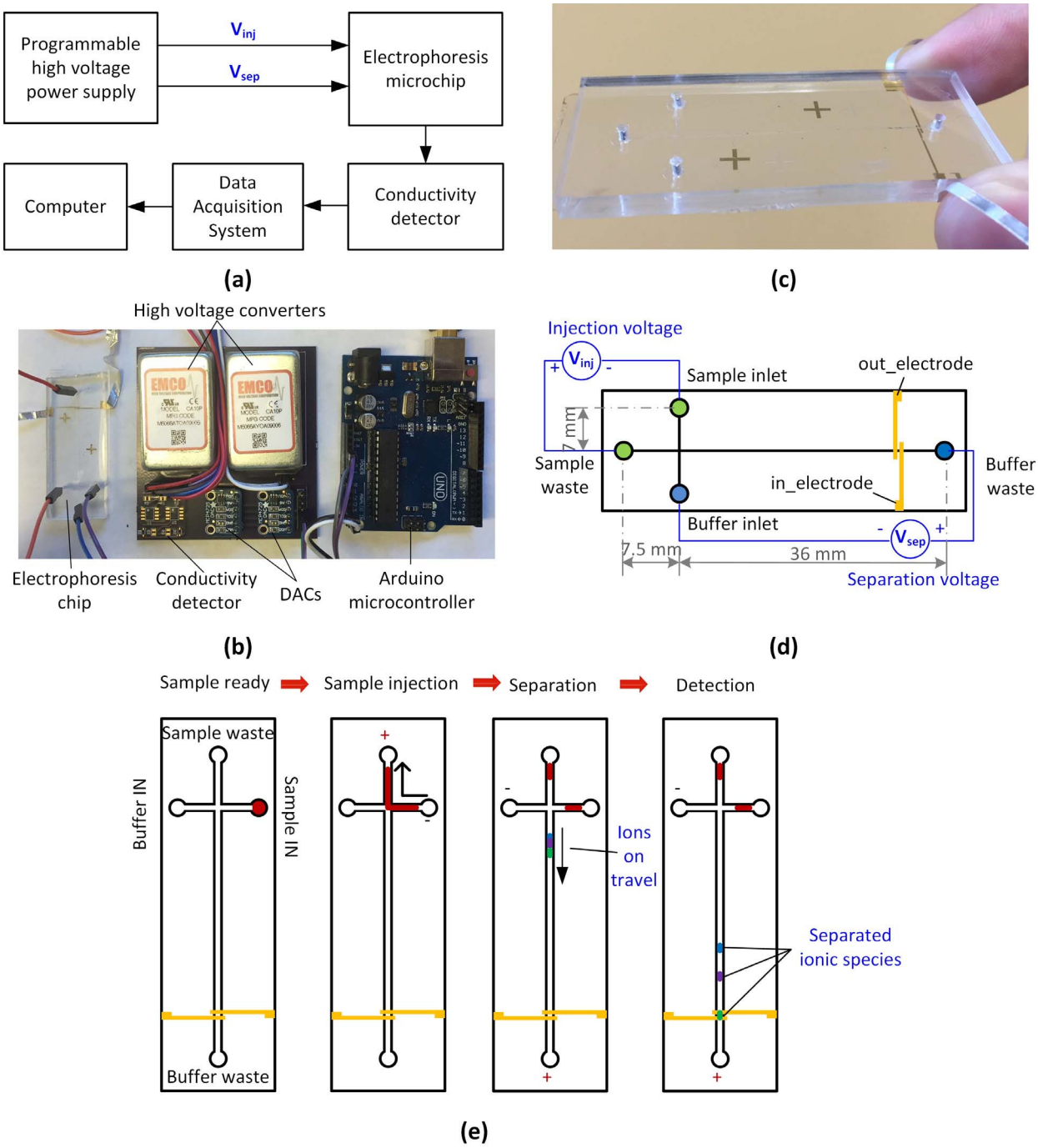

Fig. 1. (a) Schematic of the microfluidic electrophoretic ion sensor system. (b) Photograph of the developed microfluidic electrophoretic ion sensor system consisting of an electrophoresis microchip, a customized printed circuit board (PCB) integrating the two programmable precision high voltage power supply units, a conductivity detection unit, and an Arduino microcontroller. (c) Photograph of the fabricated electrophoresis microchip. (d) Schematic of an electrophoresis microchip, in_electrode is connected to the sinusoidal input and out_electrode is connected to the conductivity detection circuit. (e) Schematic of the operation steps of sampling injection, ion separation, and conductivity detection.

was also designed to enable in situ application. Different ions were separated as they travel along an electrophoretic channel under the influence of an applied electrical field, owing to their differential electrical mobilities. The sensor system includes a microfluidic electrophoresis chip with microelectrodes, a voltage application control unit, and an electrical conductivity measurement unit, all of which were designed and implemented (Fig. 1(a), (b)). A mixture of anions in the extracted soil water, including chloride (Cl^-), nitrate (NO_3^-), sulfate (SO_4^{2-}), dihydrogen phosphate ($H_2PO_4^-$), was successfully separated and detected using the developed system, showing ion separation based on travel time along the electrophoretic microchannel, with the detection peak levels corresponding to the ion concentrations. As this device required only a

minute amount of the extracted soil solution on the order of microliters, the sensor would make a negligible response to the measured environment. The detected ions contain the most important elements for plant growth, such as Nitrogen (N), Phosphorus (P), and Sulfur (S). Therefore, the developed sensing system has the potential to monitor soil's nutritional health. As mentioned above, no labeling process of analyte-recognition is necessary for the presented sensing approach. In addition, the design of the soil water solution extraction unit makes the overall system suitable for an in situ application.

II. Principle and Design

A. Principle

The electrophoretic separation of the ions in a solution takes place due to the differences in the *ion mobilities* under the influence of an applied *electric field*. The two together determine the velocity of an ion in an electrophoretic channel:

$$\upsilon = \mu_e E, \tag{1}$$

where υ is the ion velocity, μ_e is the electrophoretic mobility, and E is the applied electric field [42]. The buffer solution used in the electrophoresis microchannel also admits an electro-osmotic flow (EOF) under the influence of the same electric field [43]. The EOF is superimposed with the ionic mobility to determine an analyte's overall electrophoretic migration rate, and may reinforce or oppose it [44]. Hence, the net ion-velocity υ_{net} is:

$$\upsilon_{net} = (\mu_e \pm \mu_{EOF})E, \tag{2}$$

where μ_{EOF} denotes the EOF mobility. Accordingly, different ionic species arrive at and pass through a detector at different time points while traveling through the electrophoretic microchannel. An electrical conductivity measurement at the microelectrodes, placed at the far end of the microchannel, is a simple means to detect the arrival time and the concentrations of the separated ions. As the ions pass through the detection area, the concentrations of ionic species in the detection area change, thus changing the measured electrical conductivity. These ionic separations and the corresponding changes in the conductivity measurements show up as multiple peaks in a plot of conductivity versus time. At the low concentrations of our setting, the conductivity at any given time is given by [45]:

$$\kappa = \sum_i c_i \, |z_i| \, \lambda_i \tag{3}$$

where κ is the electrolytic conductivity measured at the electrodes, c_i is the molar concentration of the ionic species i in the solution, z_i is the ionic charge, and λ_i is the equivalent conductance of the ith ion species.

B. Electrophoretic Microchip

The designed electrophoresis microchip is shown in Fig. 1(c), with its schematic shown in Fig. 1(d). The microchip has the dimensions of 50 mm (length) × 25 mm (width) × 4 mm (height) and is made of polydimethylsiloxane (PDMS) laid over a thin 130 μm-thick glass slide that is deposited with two gold microelectrodes on the face opposite to the PDMS layer. Two perpendicular intersecting microfluidic channels are located within the PDMS layer. The shorter channel (length: 14 mm) is used for sample loading while the longer one (length: 43.5 mm) for the ion separation. Both the channels are 200 μm wide and 50 μm deep. The two gold microelectrodes, that are formed on the flip side of the glass substrate, are each 400 μm wide, and orthogonally crossed with the separation channel. The gap between the two microelectrodes is 200 μm [46]. Two sample and buffer inlets, and their corresponding outlets are located at the ends of the loading and the separation channels, respectively. Fig. 1(e) shows the fluid manipulation processes for the buffer and the analyte solutions, and to separate the ions in the analyte solution using electrophoresis.

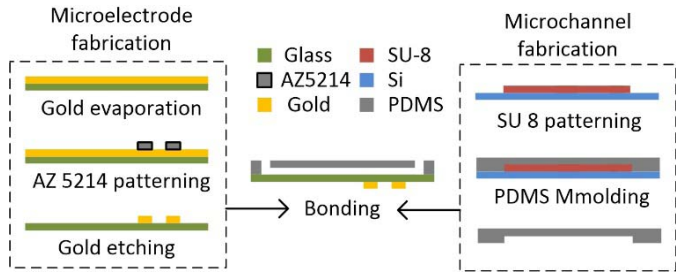

Fig. 2. Fabrication process for a microfluidic electrophoresis chip. A side view of the slice along the channel is shown.

C. Fabrication Process

The fabrication process for the microchip is schematically shown in Fig. 2. First, the detection electrode materials, consisting of 5 nm titanium and 80 nm gold, were sputtered on the surface of the thin glass substrate (60 mm × 25 mm × 0.13 mm, Superslip® cover glasses, Ted Pella, Redding, CA). Subsequently, a 1.5 μm-thick photoresist (AZ 5214, MicroChem Corp, Westborough, MA) was spin-coated on the device surface and then photo-patterned by conventional photolithography. After removal of titanium and gold from the unwanted area using an etchant solution (GE-8148, Transene, Danvers, MA), the device was flushed with acetone to thoroughly remove the remaining photoresist. Thereby, the microelectrodes were formed.

Next, separately, the PDMS microchannels were fabricated using soft lithography. For this step, a silicon wafer with photoresist SU-8 (3050; MicroChem, Westborough, MA) was spin-coated at 3000 rpm for 30 s to generate 50 μm-thick SU-8 on the surface. Then, the wafer was baked at 65 °C for 5 min and 90 °C for 1 hr. Subsequently, the wafer was exposed to an ultraviolet light with another photomask, baked at 90 °C for 30 min, and developed to form a master mold for the microfluidic channels. Following that, PDMS solution and its curing agent (Sylgard 184, Dow Corning, Auburn, MI) with a weight ratio of 10:1 was mixed, degassed, poured on the master mold and thermally cured at 70 °C for 2 hr on a hotplate. The PDMS channel layer was peeled off and necessary holes were formed using a manual punch. Finally, the thin glass substrate was bonded with the PDMS channel layer by 10 sec oxygen plasma treatment using a FEMTO Plasma Cleaner (8 psi; 100 watts; Diener Electronic, Ebhausen, Germany).

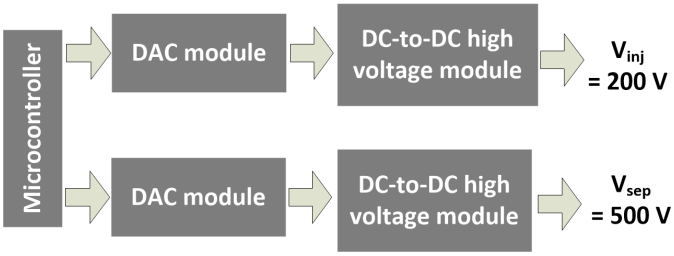

Fig. 3. A precision high voltage power supply designed to control the voltages for sample injection and ion separation.

D. Programmable High-Voltage Power Supply Unit

A programmable power supply unit was designed to provide precise electrical potentials to load a sample solution and separate ions. The unit, shown in Fig. 1b and Fig. 3, includes three main parts: Two high voltage DC to DC converters (CA10P, XP EMCO, Sutter Creek, CA), two digital to analog converters (DACs, MCP4725, Adafruit Industries, New York City, NY), and an Arduino microcontroller. The microcontroller controls the two sets of DACs and DC to DC converters, with one set providing a DC voltage V_{inj} between the sample inlet and the sample waste outlet, and the other providing another DC voltage V_{sep} between the buffer inlet and the buffer waste outlet, as shown in Fig. 1(d). Specifically, the microcontroller provides a digital control output, which is converted to an analog DC voltage between 0 and 5 V by the DAC. The DC-to-DC high voltage module elevates the low DC voltage to a high DC voltage up to 1000 V linearly. Therefore, the voltage values V_{inj} and V_{sep} can be obtained and flexibly programmed. Two pairs of electric wires are inserted into the corresponding inlets and outlets for applying the two voltages for the sample injection and the ion separation.

E. Conductivity Detection Unit

An electrical circuit model for the two microelectrodes-based detection region of the electrophoretic microchip consists of a bulk solution resistor (R_S), two parasitic capacitors (C_S) and a bypass capacitor (C_W) between the two microelectrodes, as shown in the red-dashed area of the left side of Fig. 4(a). This equivalent circuit was integrated with the conductivity detection unit, as shown in the blue-dashed areas in Fig. 4(a). The conductivity detection circuit was designed based on the principle of capacitively coupled conductivity detection [47]. The signal generator provides a sinusoidal signal of 5 mV_{p-p} on one microelectrode of the electrophoretic microchip, while its response is measured at the second microelectrode, through an I-V converter, a rectifier, and a low-pass filter. Thus, besides the sinusoidal activation, the conductivity detection circuit is used to extract, filter, amplify and transfer detected signals for analysis. The I-V convertor transforms the detected current to voltage; the voltage is rectified and low-pass filtered to suppress the "carrier" sinusoid. Two diodes are used to obtain the rectification. The resulting signal from the circuit is acquired by a multimeter.

The equivalent circuit of the two electrodes area was analyzed to obtain an equivalent impedance Z_{eq} as in Eq. (4), with its resistive and reactive values given

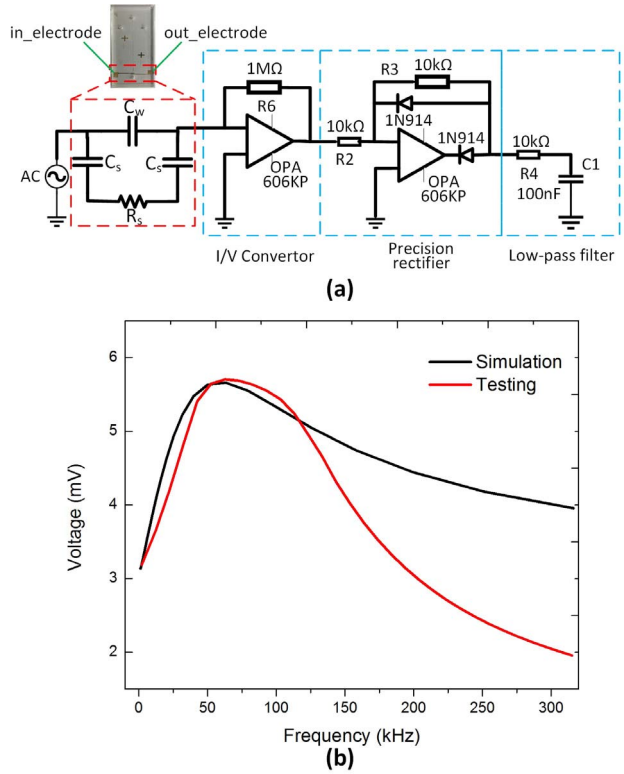

Fig. 4. (a) Conductivity detection circuit. (b) Measured versus simulated frequency responses of the microchip.

in Eqs. (5) and (6) respectively:

$$Z_{eq} = R_{eq} + jX_{eq} \tag{4}$$

$$R_{eq} = \frac{-R_s X_s X_w + R_s X_w^2}{R_s^2 + (2X_s + X_w)^2} \tag{5}$$

$$X_{eq} = \frac{X_w(4X_s^2 + 2X_s X_w + R_s^2)}{R_s^2 + (2X_s + X_w)^2} \tag{6}$$

$$X_s = -\frac{1}{\omega C_s} \tag{7}$$

$$X_w = -\frac{1}{\omega C_w}, \tag{8}$$

where R_S is the solution resistance, X_S is the parasitic reactance, X_W is the bypass reactance, and ω is the angular frequency of an applied signal.

Fig. 4(b) shows the measured and simulated magnitude frequency response of the output signal of the circuit shown in Fig. 4(a). The component values used in the simulation were identified by measurements: solution resistance, $Rs =\sim$ 140 kΩ, parasitic capacitance, $Cs =\sim$ 20 nF, and bypass capacitance, $Cw =\sim$ 0.8 nF. The maximum response was observed at 62 kHz which was chosen as the carrier sinusoid frequency to favor a high output response for the circuit.

F. Soil Solution Extraction

In additional to the electrophoretic chip and the detection unit, a vacuum-based suction unit was also designed for the in situ extraction of soil solution. This unit consists of a suction head, a poly(methyl methacrylate) or PMMA-based collection chamber, and a mini-vacuum pump (Fig. 5(a)). The suction

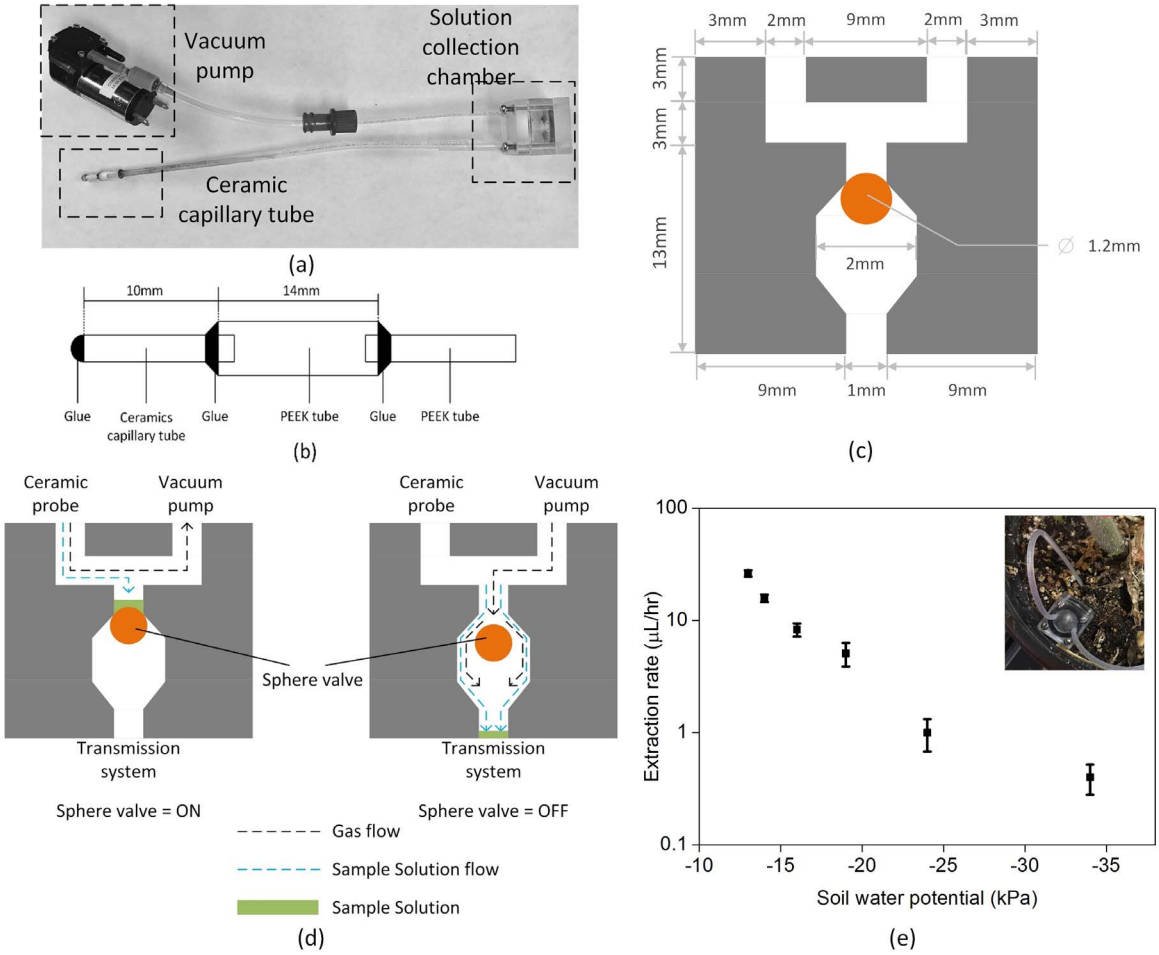

Fig. 5. (a) Schematic of the soil water extraction unit, consisting of a suction head, a PMMA chamber, and a vacuum pump. (b) Schematic of the suction head, ceramics capillary tube's outer diameter (OD) is 2.3 mm. (c) Schematic of solution collection chamber. (d) The ON and OFF working phases of the PMMA soil water collection chamber. (e) Measured extraction rates under different soil water potentials.

head structure is as shown in Fig. 5(b). A main component in the suction head is a microfiltration tubular module, consisting of a ceramic capillary tube (hydrophilic membrane composed of a blend of polyvinylpyrrolidine and polyethersulfone; mean pore size: 0.15 μm) and high pressure polyetheretherketone or PEEK tubing. The PEEK tubing of the soil water suction unit is connected with the vacuum input of the PMMA soil water collection chamber. The vacuum output is connected the vacuum pump (VMP1625MX-12-90-CH, Virtual Industries, Inc, Colorado Springs, CO, USA. Mini-Pump with 12 volt MAXON motor; flow rate: 1300mL/min; develops 18in/Hg. 16psi.). This collection chamber has an embedded plastic sphere (Fig. 5(c)). The floating sphere works as a valve and can be set to work in the ON and OFF phases (Fig. 5(d)). When the vacuum pump starts exhausting the air from the PMMA device, a low-pressure environment is built in the upper chamber, and the sphere valve gets stuck to the top end of the vertical channel, which is referred to as the "ON" mode. The system then begins to extract solution from soil through the suction head and accumulates it in the chamber atop of the sphere valve. When the extraction is completed, the pump is switched so as to fill air into the chamber. This causes the sphere to fall down, referred to as the "OFF" mode, allowing the collected solution to be delivered below (Fig 5(d)) for loading into the electrophoretic microchip.

The performance of the extraction unit was tested under different soil water potential conditions. When the soil water potential was high, which means wet soil, the extraction rate was also high (e.g., 26.3 $\pm$ 1.73 μL/hr at -13 kPa). The extraction rate dropped significantly with decreasing soil water potential (Fig. 5(e)).

III. Electrophoretic Chip Testing

The buffer solution used for on-chip electrophoresis was chosen to be 2-[N-Morpholino]ethanesulfonic acid (MES)/ Histidine (HIS) 30 mM/30 mM, with 4 mmol 18-crown-6 and 0.1% methyl cellulose at 6.0 pH [47]. Both synthetic and extracted soil sample solutions were tested. The synthetic solution included a mixture of KNO_3 and Na_2SO_4 (each with 50 μM) in deionized (DI) water to evaluate the ability of the sensor to separate different ions, and different concentration solutions of KNO_3 in DI water to test the ability of the sensor to quantify nitrate ion concentrations.

Two types of real samples were prepared. The real sample of the first type (Type 1) was extracted from the soil samples collected at different locations of a *Z.mays* (type of maize) farm field at the Agricultural Engineering and Agronomy Research Farm (Boone, Iowa). Briefly, 10 g of field moist soil was weighed in a specimen cup. 50 mL of DI water was then added to the specimen cup and shaken on a reciprocal shaker for 1 hr. After shaking, the solution was filtered using Whatman #1 filter paper and the filtrates were collected, diluted with DI water at ratio 1 to 10, and stored at 4 °C until taken out for injection into the electrophoretic microchip [48].

The real sample solution of the second type (Type 2) was collected directly from soils by the presented soil solution extraction unit. The suction head was insert into the soil, with the extraction unit running for 1 hour to extract about 20 μL of soil solution under the soil water potential of -13 kPa.

To perform the ion concentration measurement on the electrophoretic microchip, the MES/HIS buffer solution was loaded into both the microfluidic channels by using a 3 mL syringe (Becton Dickinson, NJ, USA) with a microbore tubing (Cole-Parmer, IL, USA). Subsequently, a specific sample solution was placed at the inlet of the microchip using a pipette (Thermo Scientific, MA, USA). Next, the sample solution was injected into the shorter channel by generating and applying a 200 V between the sample inlet and the sample waste outlet for 6 sec to allow filling the intersection. Subsequently, ion separation was carried out by applying 500 V between the buffer reservoir and the buffer waste reservoir for 450 sec. The conductivity detection at the electrode was performed using a 5 mV_{p-p} excitation voltage at 62 kHz. After each test-run, the microchip was rinsed with 1 mL buffer solution for 10 times.

IV. Results and Discussion

A. Separation of Ions

Fig. 6 shows the output voltage of the microchip system over a period of 300 sec when the device was used to separate the anions of NO_3^- and SO_4^{2-} (50 μM each) present in the synthetic sample solution. The experimental result clearly shows two voltage peaks at two different times owing to different ionic mobilities of the NO_3^- and SO_4^{2-} ions. Note while the concentrations of the two ions were the same in the synthetic sample solution, their peak intensities were different, owing to the differences in their changes and ionic conductivities.

B. Sensitivity and Detection-Limit From Single Ion Detection

For the sensitivity and the detection-limit analysis, nitrate sensing was performed using the synthetic nitrate solutions of concentrations 20, 40, 60, 80, and 100 mM. Each solution was loaded into the same microchip for 3 different detection runs. Fig. 7(a) shows the peaks corresponding to 20, 40, 60, 80, and 100 μM of nitrate ion concentrations, all of which appeared around the same time (187 ± 3 s), indicating the high temporal accuracy of the sensor for a given ion species. Furthermore, the five nitrate concentrations can be clearly distinguished by their corresponding peak levels. Fig. 7(b) demonstrates that the voltage output of the sensor is almost linear to the input nitrate concentration. A linear fit of the data (Fig. 7(b)) indicates that the sensitivity of the sensor for the detection of the nitrate ions is approximately 0.0915 mV/μM.

The limit of detection (LOD) of the presented sensor is defined to be three times the standard deviation over the

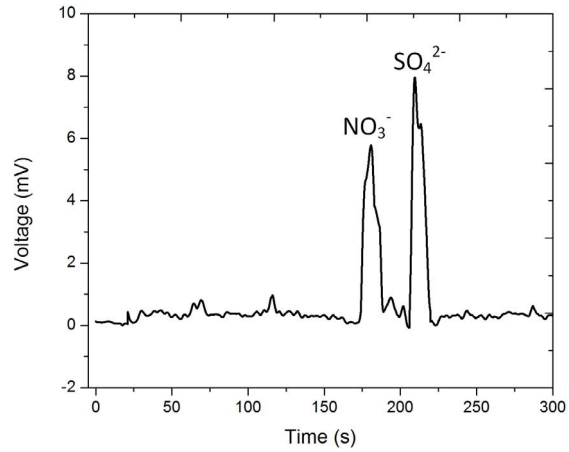

Fig. 6. Experimental results for separation of NO_3^- from SO_4^{2-} ions in the synthetic sample solution containing only these two ion species.

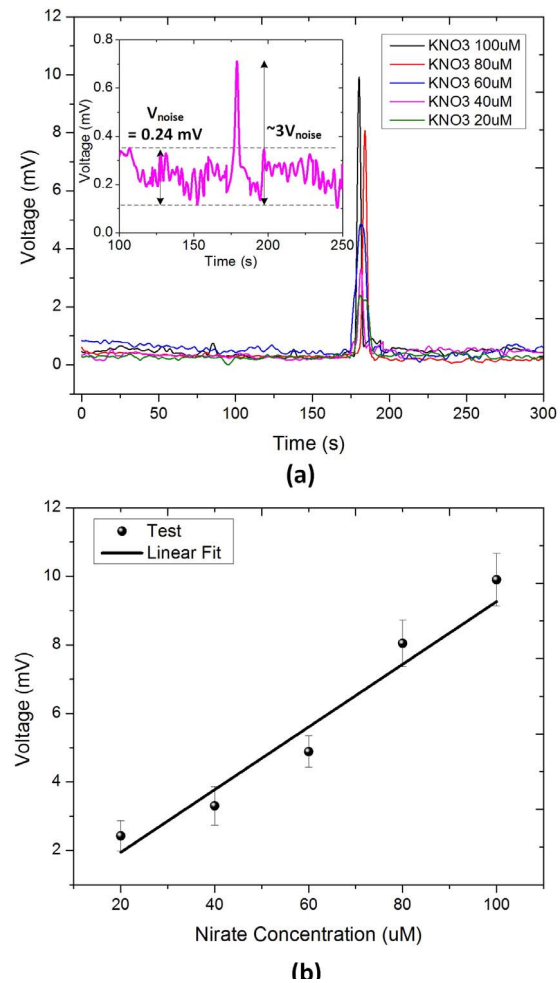

Fig. 7. (a) Experimental voltage response of the electrophoresis chip over a period of 300 s to different nitrate ion concentrations. (b) Output voltage of the sensor as a function of nitrate ion concentration.

average of the voltage readout, in the absence of any analyte. The noise floor of the sensor is 0.30 ± 0.12 mV. Therefore, according to the above-mentioned definition, the LOD of the sensor is equivalent to a nitrate concentration that will result in an output voltage of $0.3 + (3 \times 0.12)$ mV $=$ 0.66 mV. This corresponds to LOD of around 7.25 μM. As shown in the inset of Fig. 7(a), it is also confirmed that the minimum detectable nitrate concentration of this sensor is 7.25 μM, which is an improvement compared to some previously reported values [50], and much lower than the amount found in agricultural soil. While this LOD is slightly higher than some ISE-based and enzymatic electrochemical sensors [26], the electrophoretic sensor has the advantage of being label-free, thereby eliminating the limit on sensor life due to the limited life of the ion selective materials.

C. Soil Solution Testing

The developed sensor was used to detect the major anions in the two types of real sample solutions collected from the soils. As mentioned in Section III, the first-type soil sample solution was obtained through the standard shaking and filtering process, and the second-type soil sample solution was collected directly by the developed extraction unit. Fig. 8 shows the result corresponding to the separated anions, under the applied electrical field, detected as time-separated voltage peaks, and served as a proof-of-principle.

In order to identify the ion types corresponding to the observed peaks, we tested four types of standard solutions independently using the microchip, each solution included only a single type of anion: chloride (Cl^-), nitrate (NO_3^-), sulphate ($SO4^{2-}$), and dihydrogen phosphate ($H_2PO_4^-$), respectively (Fig. 8 (a)). These included the three important nutrients (nitrogen, phosphorus, and sulphur), plus chlorine that is considered to be the main interfering species for nitrogen. Although there are more than 4 peaks, especially in the solution extracted using a standard method, at this point only the four ions were cared to identify, for demonstrating a proof-of-principle. As discussed below, the 0.15 μm mean pore size of the extraction unit's suction head is able to filter out many extraneous particles/microbes.

The measured peaks for the 4 known ions were mapped against the results of the soil sample solution tests (Fig 8(b) (c)). The difference between plots in Fig. 8(b) versus in Fig. 8(c) revealed a notable fact that the different extraction methods can yield different number of ion species. In fact, the ones present in the solution obtained through a standard extraction method (in Fig. 8(b)) are not the same as the ones available to the plants. On the other hand, since the soil solution extraction unit works on the principle of the water potential difference, and which is how the plants are also able to ingest nutrients, the solution extracted using the extraction unit provides a more realistic picture of what soil ions may be available to the plants. Furthermore, since the pore size (0.15 μm) of the suction head used in the extraction unit is much smaller than the pore size of Whatman #1 filter paper (11 μm) used in the standard solution extraction method, more extraneous particles/microbes were filtered out by the extraction unit, which also explains the fewer number of detected peaks in the solution extracted by the suction unit.

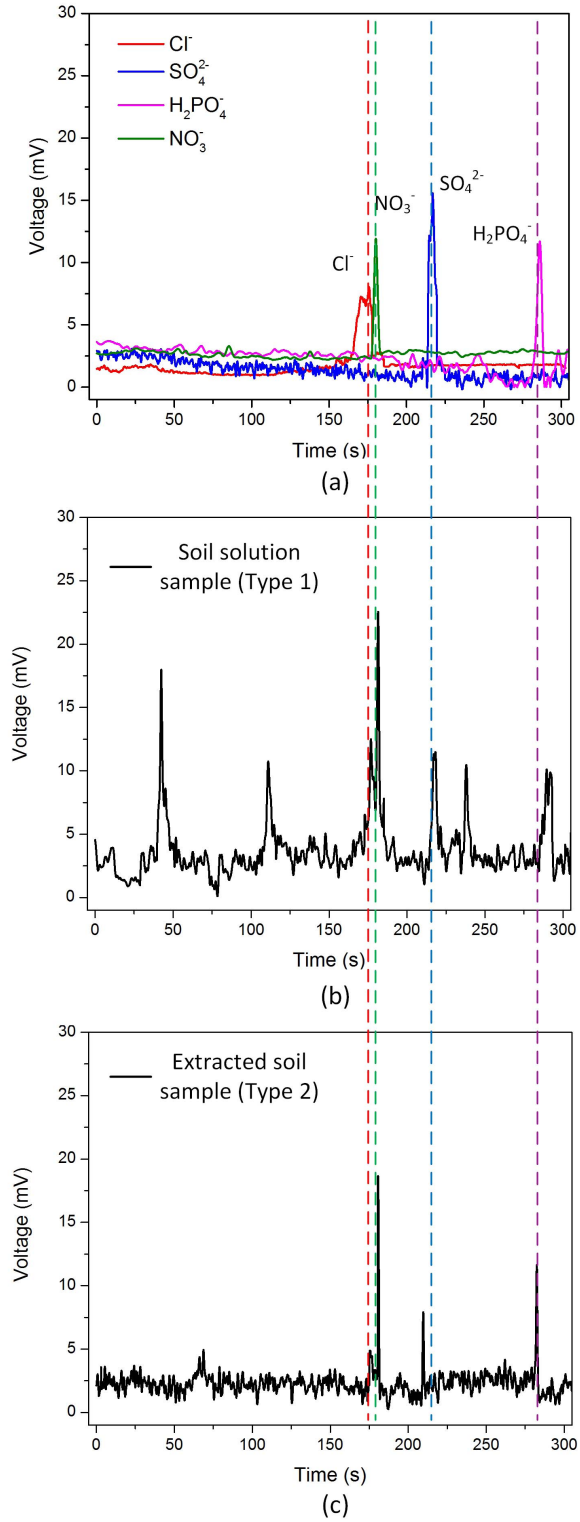

Fig. 8. Electropherograms of the device showing the separation and detection of anions in different samples: (a) four synthetic samples with each containing only a single anion species (Cl^-, NO_3^-, $SO4^{2-}$, or $H_2PO_4^-$); (b) real soil solution sample of the first type prepared using the standard shaking and filtering method; and (c) the real sample solution of the second type directly extracted from the soil using the extraction unit. It has less peaks because the smaller pore filter removes many of the particulate matters and microbes.

Using the result of mapping of the plots corresponding to the 4 known ion types against those of the two extracted solutions (Fig. 8(b)(c)), the peaks were labeled in Fig. 8 accordingly.

It is clear from the figure that the four ions in questions could be separated from each other, including nitrogen from chlorine. Furthermore, using the calibration plot in Fig. 7(b), the detected nitrate concentration in the soil sample was found to be 210.3 ± 3.52 μM, which is within a 9% error-margin of the concentration value $191.2 \pm 2.39\mu$M obtained using a sophisticated benchtop ultraviolet spectrophotometer. The slightly higher measured value for nitrate can be understood as follows: due to the closeness of the mobilities of chloride and nitrate (as noted from the proximity of their peaks), some residual chloride ions passed through the detection area while the nitrate ions started to go through that area, resulting in a slightly enhanced signal. In order to correct for such enhancement due to the overlap of the ions, one possible method would be to mathematically characterize the overlap, and algorithmically correct the reported value of the nitrate concentration. Another approach would be to increase the length of the separation channel to allow a larger gap between the two peaks and their better separation. Both these approaches are directions for future research.

V. Conclusion

A microfluidic microchip nutrient sensing system was developed to extract, separate, detect, and quantify nutrient ions in soil sample solutions. The system can be used for extracting and testing analytes from other sources (e.g., water). Using this system, a mixture of anions present in the soil solution extracted using the new suction unit as well as from an existing standard method was separated and detected via distinguishing peaks, separated over time. Further, a good linear relation between a single ion (nitrate) concentration and detected signal peak was demonstrated. This together with a limit of detection of $\sim$7.25 μM for nitrate ions demonstrated a good performance of the proposed detection system. The design and implementation of the soil solution extraction unit makes the entire sensing system suited for in situ applications. The extraction unit is driven by the water potential gradient, matching how the plants ingest nutrients, unlike the standard soil solution extraction methods. Also the smaller-sized pores in the suction heads ensures that many of the impurities (particles/microbes) are automatically filtered out. In order to make the sensing system fully ready for an in situ adoption, it would additionally require its integration with a wireless communication unit, such as one reported in [4]. A fully integrated sensing system has great prospects in nutrient management for precision farming.

Future research work would include (i) integrating the electrophoretic microchip sensor system with the soil solution extraction unit, a pumping unit for delivery of buffer solution and waste, external storage and waste reservoirs, and a wireless communication capability to realize a finished prototype for in situ soil nutrient monitoring, (ii) improving the microchip design, e.g., thinning down the glass substrate to further increase the output signal strength and thereby the sensitivity and LOD, (iii) optimizing the detection circuit to reduce noise floor and thus further lowering the detection limit of the system, and (iv) expanding the ability of the device to detect and quantify also the cations besides the anions.

Acknowledgment

The authors thank Navreet Mahal, and Dr. Michael Castellano of the Agronomy Department at ISU for assistance with soil sample extraction and testing.

References

[1] A. Bah, S. K. Balasundram, and M. H. A. Husni, "Sensor technologies for precision soil nutrient management and monitoring," *Amer. J. Agricult. Biol. Sci.*, vol. 7, no. 1, pp. 43–49, Jan. 2012.

[2] K. Goulding, S. Jarvis, and A. Whitmore, "Optimizing nutrient management for farm systems," *Philos. Trans. Roy. Soc. B, Biol. Sci.*, vol. 363, no. 1491, pp. 667–680, Feb. 2008.

[3] H. Sahota, R. Kumar, and A. Kamal, "A wireless sensor network for precision agriculture and its performance," *Wireless Commun. Mobile Comput.*, vol. 11, no. 12, pp. 1628–1645, Dec. 2011.

[4] J. Huang, R. Kumar, A. Kamal, and R. Weber, "Development a wireless soil sensor network," in *Proc. Amer. Soc. Agricult. Biosyst. Eng.*, Providence, RI, USA, Jun. 2008, pp. 1–9.

[5] P. C. Robert, "Precision agriculture: A challenge for crop nutrition management," *Plant Soil*, vol. 247, no. 1, pp. 143–149, Nov. 2002.

[6] N. Zhang, M. Wang, and N. Wang, "Precision agriculture—A worldwide overview," *Comput. Electron. Agricult.*, vol. 36, nos. 2–3, pp. 113–132, Nov. 2002.

[7] C.-H. Ho, S.-H. Lin, H.-C. Hu, and Y.-F. Tsay, "CHL1 functions as a nitrate sensor in plants," *Cell*, vol. 138, no. 6, pp. 1184–1194, Sep. 2009.

[8] G. Pandey, R. Kumar, and R. J. Weber, "A low RF-band impedance spectroscopy based sensor for *in situ*, wireless soil sensing," *IEEE Sensors J.*, vol. 14, no. 6, pp. 1997–2005, Jun. 2014.

[9] F. Kizito *et al.*, "Frequency, electrical conductivity and temperature analysis of a low-cost capacitance soil moisture sensor," *J. Hydrol.*, vol. 352, no. 3, pp. 367–378, May 2008.

[10] S. Staggenborg, M. A. Carignano, and L. Haag, "Predicting soil pH and buffer pH *in situ* with a real-time sensor," *Agronomy J.*, vol. 99, no. 3, pp. 854–861, May 2007.

[11] T. Jackson, K. Mansfield, M. Saafi, T. Colman, and P. Romine, "Measuring soil temperature and moisture using wireless MEMS sensors," *Measurement*, vol. 41, no. 4, pp. 381–390, May 2008.

[12] Z. Zou *et al.*, "Environmentally friendly disposable sensors with microfabricated on-chip planar bismuth electrode for *in situ* heavy metal ions measurement," *Sens. Actuators B, Chem.*, vol. 134, no. 1, pp. 18–24, Aug. 2008.

[13] J. V. Sinfield, D. Fagerman, and O. Colic, "Evaluation of sensing technologies for on-the-go detection of macro-nutrients in cultivated soils," *Comput. Electron. Agric.*, vol. 70, no. 1, pp. 1–18, Jan. 2010.

[14] D. L. Corwin and S. M. Lesch, "Apparent soil electrical conductivity measurements in agriculture," *Comput. Electron. Agricult.*, vol. 46, nos. 1–3, pp. 11–43, Mar. 2005.

[15] K. A. Sudduth, S. T. Drummond, and N. R. Kitchen, "Accuracy issues in electromagnetic induction sensing of soil electrical conductivity for precision agriculture," *Comput. Electron. Agricult.*, vol. 31, no. 3, pp. 239–264, May 2001.

[16] E. Ben-Dor and A. Banin, "Near-infrared analysis as a rapid method to simultaneously evaluate several soil properties," *Soil Sci. Soc. Amer. J.*, vol. 59, no. 2, pp. 364–372, Mar. 1995.

[17] J. Reeves, G. McCarty, and T. Mimmo, "The potential of diffuse reflectance spectroscopy for the determination of carbon inventories in soils," *Environ. Pollution*, vol. 116, pp. S277–S284, Mar. 2002.

[18] R. Verschoore, J. G. Pieters, T. Seps, Y. Spriet, and J. Vangeyte, "Development of a sensor for continuous soil resistance measurement," in *Precision Agriculture*. Wageningen, The Netherlands: Academic, 2003, pp. 689–695.

[19] T. E. Grift, M. Z. Tekeste, and R. L. Raper, "Acoustic compaction layer detection," *Trans.-Amer. Soc. Agricult. Eng.*, vol. 48, no. 5, pp. 1723–1730, 2005.

[20] S. J. Birrell and J. W. Hummel, "Multi-sensor ISFET system for soil analysis," *Precis. Agricult.*, vol. 97, pp. 459–468, Sep. 1997.

[21] D. L. Jones, "Organic acids in the rhizosphere—A critical review," *Plant Soil*, vol. 205, no. 1, pp. 25–44, Aug. 1998.

[22] C.-W. Chang, D. A. Laird, M. J. Mausbach, and C. R. Hurburgh, "Near-infrared reflectance spectroscopy–principal components regression analyses of soil properties," *Soil Sci. Soc. Amer. J.*, vol. 65, no. 2, pp. 480–490, Mar. 2001.

[23] R. R. Price, J. W. Hummel, S. J. Birrell, and I. S. Ahmad, "Rapid nitrate analysis of soil cores using ISFETs," *Trans. Amer. Soc. Agricult. Eng.*, vol. 46, no. 3, pp. 601–610, 2003.

[24] E. Bakker and M. Telting-Diaz, "Electrochemical sensors," *Anal. Chem.*, vol. 74, no. 12, pp. 2781–2800, Jun. 2002.

[25] M. A. Ali *et al.*, "Tunable bioelectrodes with wrinkled-ridged graphene oxide surfaces for electrochemical nitrate sensors," *RSC Adv.*, vol. 6, no. 71, pp. 67184–67195, Jul. 2016.

[26] A. T. Woolley, D. Hadley, P. Landre, A. J. deMello, R. A. Mathies, and M. A. Northrup, "Functional integration of PCR amplification and capillary electrophoresis in a microfabricated DNA analysis device," *Anal. Chem.*, vol. 68, no. 23, pp. 4081–4086, Dec. 1996.

[27] M. W. Lada, T. W. Vickroy, and R. T. Kennedy, "High temporal resolution monitoring of glutamate and aspartate *in vivo* using microdialysis on-line with capillary electrophoresis with laser-induced fluorescence detection," *Anal. Chem.*, vol. 69, no. 22, pp. 4560–4565, Nov. 1997.

[28] C. S. Effenhauser, G. J. M. Bruin, A. Paulus, and M. Ehrat, "Integrated capillary electrophoresis on flexible silicone microdevices: Analysis of DNA restriction fragments and detection of single DNA molecules on microchips," *Anal. Chem.*, vol. 69, no. 17, pp. 3451–3457, Sep. 1997.

[29] C. L. Colyer, T. Tang, N. Chiem, and D. J. Harrison, "Clinical potential of microchip capillary electrophoresis systems," *Electrophoresis*, vol. 18, no. 10, pp. 1733–1741, Apr. 1997.

[30] Y. Huang *et al.*, "Electric manipulation of bioparticles and macromolecules on microfabricated electrodes," *Anal. Chem.*, vol. 73, no. 7, pp. 1549–1559, Feb. 2001.

[31] Z. Liang, N. Chiem, G. Ocvirk, T. Tang, K. Fluri, and D. J. Harrison, "Microfabrication of a planar absorbance and fluorescence cell for integrated capillary electrophoresis devices," *Anal. Chem.*, vol. 68, no. 6, pp. 1040–1046, Mar. 1996.

[32] M. Albin, R. Weinberger, E. Sapp, and S. Moring, "Fluorescence detection in capillary electrophoresis: Evaluation of derivatizing reagents and techniques," *Anal. Chem.*, vol. 63, no. 5, pp. 417–422, Mar. 1991.

[33] J. Webster, M. A. Burns, D. T. Burke, and C. H. Mastrangelo, "Monolithic capillary electrophoresis device with integrated fluorescence detector," *Anal. Chem.*, vol. 73, no. 7, pp. 1622–1626, Apr. 2001.

[34] M. L. Chabinyc *et al.*, "An integrated fluorescence detection system in poly (dimethylsiloxane) for microfluidic applications," *Anal. Chem.*, vol. 73, no. 18, pp. 4491–4498, Sep. 2001.

[35] C. Dongre, H. J. Hoekstra, and M. Pollnau, "Capillary electrophoresis and multicolor fluorescent DNA analysis in an optofluidic chip," in *Capillary Electrophoresis and Microchip Capillary Electrophoresis: Principles, Applications, and Limitations*. Hoboken, NJ, USA: Wiley, 2013, pp. 247–266.

[36] H. Craighead, "Future lab-on-a-chip technologies for interrogating individual molecules," *Nature*, vol. 442, no. 7101, pp. 387–393, Jul. 2006.

[37] D. R. Reyes, D. Iossifidis, P. A. Auroux, and A. Manz, "Micro total analysis systems. 1. Introduction, theory, and technology," *Anal. Chem.*, vol. 74, no. 12, pp. 2623–2636, Jun. 2002.

[38] P.-A. Auroux, D. Iossifidis, D. R. Reyes, and A. Manz, "Micro total analysis systems. 2. Analytical standard operations and applications," *Anal. Chem.*, vol. 74, no. 12, pp. 2637–2652, Jun. 2002.

[39] A. T. Woolley and R. A. Mathies, "Ultra-high-speed DNA fragment separations using microfabricated capillary array electrophoresis chips," *Proc. Natl. Acad. Sci. USA*, vol. 91, no. 24, pp. 11348–11352, Nov. 1994.

[40] M. Smolka *et al.*, "A mobile lab-on-a-chip device for on-site soil nutrient analysis," *Precision Agricult.*, vol. 18, no. 2, pp. 152–168, Apr. 2017.

[41] T. Kappes, B. Galliker, M. A. Schwarz, and P. C. Hauser, "Portable capillary electrophoresis instrument with amperometric, potentiometric and conductometric detection," *TrAC Trends Anal. Chem.*, vol. 20, no. 3, pp. 133–139, Mar. 2001.

[42] E. O. Knutson and K. Whitby, "Aerosol classification by electric mobility: Apparatus, theory, and applications," *J. Aerosol Sci.*, vol. 6, no. 6, pp. 443–451, Nov. 1975.

[43] G. F. Yao, "A computational model for simulation of electroosmotic flow in microsystems," in *Proc. Nanotechnol. Conf. Trade Show*, 2003, vol. 1, no. 9, pp. 218–221.

[44] V. M. Ugaz and J. L. Christensen, "Electrophoresis in microfluidic systems," in *Microfluidic Technologies for Miniaturized Analysis Systems*. New York, NY, USA: Springer, 2007, pp. 393–438.

[45] M. R. Wright, "Conductance: The ideal case," in *An Introduction to Aqueous Electrolyte Solutions*, Hoboken, NJ, USA: Wiley, 2007, pp. 421–474.

[46] F. Opekar, P. Tůma, and K. Štulík, "Contactless impedance sensors and their application to flow measurements," *Sensors*, vol. 13, no. 3, pp. 2786–2801, 2013.

[47] J. A. F. da Silva and C. L. do Lago, "An oscillometric detector for capillary electrophoresis," *Anal. Chem.*, vol. 70, no. 20, pp. 4339–4343, Sep. 1998.

[48] P. Schmitt-Kopplin, "Determination of small ions with capillary electrophoresis and contactless conductivity detection," in *Capillary Electrophoresis* (Methods Protocols). Totowa, NJ, USA: Humana Press, 2008, pp. 3–19.

[49] R. Hood-Nowotny, N. H.-N. Umana, E. Inselbacher, P. Oswald-Lachouani, and W. Wanek, "Alternative methods for measuring inorganic, organic, and total dissolved nitrogen in soil," *Soil Sci. Soc. Amer. J.*, vol. 74, pp. 1018–1027, May 2010.

[50] P. Kubáň and P. C. Hauser, "Application of an external contactless conductivity detector for the analysis of beverages by microchip capillary electrophoresis," *Electrophoresis*, vol. 26, no. 16, pp. 3169–3178, Aug. 2005.

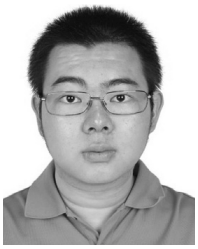

Zhen Xu received the B.S. degree from Tsinghua University, Beijing, China, in 2011. He is currently pursuing the Ph.D. degree with the Department of Electrical and Computer Engineering, Iowa State University. His current research interests include developing MEMS and microfluidic devices and sensors for sustainable agriculture.

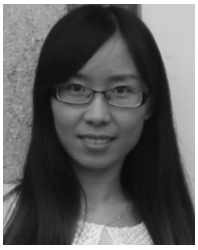

Xinran Wang received the B.S. degree in electrical engineering from Wuhan University, China, in 2011, and the M.S. degree from the Wuhan Institute of Physics and Mathematics, China Academy of Sciences, in 2014. She is currently pursuing the Ph.D. degree in electrical engineering with Iowa State University. Her research interests include sensors, electronics, and biochips for sustainable agriculture.

Robert J. Weber began his prolific career in the Solid State Research Laboratory, Collins Radio Company, later a part of Rockwell International. For 25 years, he was involved in advanced development and applied research in the one-to-ten-GHz frequency range and received several distinguished awards for his valuable contributions to this field. He has taught microwave circuit design and fiber-optics communications with the Department of Electrical and Computer Engineering, Iowa State University. He is currently involved in ongoing experimental research in integrating microwave circuits with other devices, such as energy harvesters, MEMS, electronic and chemical sensors, and electro-optics.

Ratnesh Kumar (F'07) received the B.Tech. degree in electrical engineering from IIT Kanpur, India, and the M.S. and Ph.D. degrees in electrical and computer engineering from the University of Texas, Austin, TX, USA, in 1987, 1989, and 1991, respectively. He was on faculty with the University of Kentucky from 1991 to 2002 in electrical and computer engineering, and has held visiting positions with the University of Maryland, the Applied Research Laboratory (at Penn State University), NASA Ames, the Idaho National Laboratory, the United Technologies Research Center, and the Air Force Research Laboratory. He has been a Professor of Electrical and Computer Engineering with Iowa State University since 2002. He received the Gold Medals for the Best EE Undergrad and the Best All Rounder from IIT Kanpur, and the Best Dissertation Award from UT Austin. He is a Distinguished Lecturer for the IEEE Control Systems Society. He received the Best Paper Award from the IEEE TRANSACTIONS ON AUTOMATION SCIENCE AND ENGINEERING.

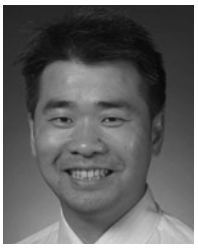

Liang Dong received the Ph.D. degree in electronic science and technology from the Institute of Microelectronics, Tsinghua University, Beijing, China, in 2004. From 2004 to 2007, he was a Post-Doctoral Research Associate with the Department of Electrical and Computer Engineering, University of Wisconsin–Madison. He has a courtesy appointment at the Iowa State's Department of Chemical and Biological Engineering and is an Associate of the DOE's Ames Laboratory. In 2014, he was selected as a Faculty Scholar of the Plant Sciences Institute, Iowa State University. He is currently an Associate Professor with the Department of Electrical and Computer Engineering, Iowa State University. His current research interests include MEMS, microfluidics, sensors, nanophotonics, and micro/nanomanufacturing and their applications in sustainable agriculture and environments, plant sciences, biomedicine, and Internet of Things. He serves as an Editorial Board Member for Scientific Reports and is a Guest Editor of *Micromachines*. He received the National Science Foundation CAREER Award, the Early Career Engineering Faculty Research Award, the Harpole-Pentair Developing Faculty Award, and the Warren B. Boast Undergraduate Teaching Award at Iowa State University. Before he came to the U.S., he received the Top 100 National Outstanding Doctoral Dissertation Award in China, and the Academic Rising Star Award from Tsinghua University.